APPLIED AND ENVIRONMENTAL MICROBIOLOGY, Aug. 2003, p. 4474–4481 Vol. 69, No. 8
0099-2240/03/$08.00+0 DOI: 10.1128/AEM.69.8.4474–4481.2003

Role of Capsular Colanic Acid in Adhesion of Uropathogenic *Escherichia coli*

Andrea Hanna,[1]† Michael Berg,[2,3] Valerie Stout,[2,3] and Anneta Razatos[1,3]*

Department of Chemical and Materials Engineering,[1] Department of Microbiology,[2] and The Molecular and Cellular Biology Program,[3] Arizona State University, Tempe, Arizona

Received 16 January 2003/Accepted 6 May 2003

Urinary tract infections are the most common urologic disease in the United States and one of the most common bacterial infections of any organ system. Biofilms persist in the urinary tract and on catheter surfaces because biofilm microorganisms are resistant to host defense mechanisms and antibiotic therapy. The first step in the establishment of biofilm infections is bacterial adhesion; preventing bacterial adhesion represents a promising method of controlling biofilms. Evidence suggests that capsular polysaccharides play a role in adhesion and pathogenicity. This study focuses on the role of physiochemical and specific binding interactions during adhesion of colanic acid exopolysaccharide mutant strains. Bacterial adhesion was evaluated for isogenic uropathogenic *Escherichia coli* strains that differed in colanic acid expression. The atomic force microscope (AFM) was used to directly measure the reversible physiochemical and specific binding interactions between bacterial strains and various substrates as bacteria initially approach the interface. AFM results indicate that electrostatic interactions were not solely responsible for the repulsive forces between the colanic acid mutant strains and hydrophilic substrates. Moreover, hydrophobic interactions were not found to play a significant role in adhesion of the colanic acid mutant strains. Adhesion was also evaluated by parallel-plate flow cell studies in comparison to AFM force measurements to demonstrate that prolonged incubation times alter bacterial adhesion. Results from this study demonstrate that the capsular polysaccharide colanic acid does not enhance bacterial adhesion but rather blocks the establishment of specific binding as well as time-dependent interactions between uropathogenic *E. coli* and inert substrates.

Urinary tract infections (UTIs) are the most common urologic disease in the United States and one of the most common bacterial infections of any organ system (40). UTIs are especially common in cases of catheterization. The incidence of infection in patients with indwelling catheters increases 5 to 10% per day (4, 41). Within 3 weeks of use, 100% of patients with indwelling catheters will acquire UTIs due to the establishment of biofilms on the catheter material (4, 24). Scanning electron microscopy has shown that most catheters removed from patients after only 7 days are colonized by bacterial biofilms (4). Biofilms persist in the urinary tract and on catheter surfaces because the microorganisms contained within a biofilm are well protected from urine flow and host defense mechanisms (19, 24). More importantly, bacteria within biofilms are strongly resistant to antibiotic therapy (11–13, 17). In light of the growing resistance of bacteria to antibiotics, one promising approach to treat catheter infections is to prevent the formation of biofilms by blocking the first step—bacterial adhesion.

Development of infection-resistant materials and treatments requires detailed knowledge of the factors and forces involved in bacterial adhesion. Bacterial adhesion is governed by reversible physiochemical forces that include electrostatic, van der Waals, and hydrophobic interactions, followed by the establishment of irreversible interactions such as specific receptor-ligand binding events (1, 8, 11, 17, 23). Previous studies have shown that molecules expressed on the bacterial cell surface influence the physiochemical interactions between bacteria and substrates during reversible physiochemical adhesion (32). Moreover, specific binding of bacteria to substrates is believed to be mediated by polymeric molecules on the bacterial cell surface, such as pili, fimbriae, lipopolysaccharides, or capsular polysaccharides (1, 11, 23, 27). At the present time, the role of these important cell surface molecules in reversible physiochemical and specific binding interactions is poorly understood. The goal of this study is to quantitatively evaluate the role of colanic acid in bacterial adhesion. Colanic acid is a negatively charged polymer of glucose, galactose, fucose, and glucuronic acid that forms a protective capsule surrounding the bacterial cell surface. Previous studies have shown that colanic acid synthesis is up-regulated in biofilms (14, 29), whereas it is well known that colanic acid is not synthesized in planktonic cells under normal laboratory growth conditions. Evidence suggests that capsular polysaccharides play a role in pathogenicity (9, 10, 15). The expression of colanic acid has also been shown to be required for the creation of normal *Escherichia coli* biofilm architecture (14). However, these studies also indicate that colanic acid expression is not relevant to the initial adhesion events (14). Our research focuses on the initial stages of adhesion (<30 min) to various surfaces, using uropathogenic *E. coli* strains, whereas previous studies evaluated the role of colanic acid in adhesion of *E. coli* K-12 strains to polyvinyl chloride after extended incubation times (>10 h) with the surface (14). This is the first report of the adherence properties of a fully encapsulated strain compared with those of a wild-type strain and a strain incapable of making a capsule. Our research indicates that the initial interaction forces be-

* Corresponding author. Mailing address: Department of Chemical Engineering, ASU, P.O. Box 876006, Tempe, AZ 85287-6006. Phone: (480) 965-0874. Fax: (480) 965-0037. E-mail: razatos@asu.edu.
† Present address: Intel Corporation, Santa Clara, CA 95052.

TABLE 1. Uropathogenic *E. coli* strains

Strain	Relevant enotype	Colanic acid expression	OmpC expression	Source or reference
C97 parent strain		Wild type	+	22
CPS$^-$	*cpsE*::Tn*10*	Minus	+	C97 + P1(SG20043)
CPS wild type	*ompC*::Tn*5*	Wild type	−	C97 + P1(SG20803)
CPS$^+$	rcsC137 *ompC*::Tn*5*	Plus	−	C97 + P1(SG20803)
SG20043	*cpsE*::Tn*10* Δ*lon-100*	Minus	+	37
SG20803	rcsC137 *ompC*::Tn*5*	Plus	−	3

tween bacteria and the surface change with extended exposure to the surface.

Bacterial adhesion was evaluated in this study for uropathogenic *E. coli*, which is the principle causative agent of both acute and catheter-associated UTIs (7, 39, 40). The atomic force microscope (AFM) was used to directly measure the reversible physiochemical and specific binding interactions between bacteria and various substrates as bacteria initially approach the interface. Bacterial adhesion was also evaluated in parallel-plate flow cell studies to investigate the influence of colanic acid on bacterial adhesion during prolonged incubation times in comparison to AFM force measurements, which are instantaneous. Results from this study will ultimately be used to direct the development of adhesion-resistant materials and methods to reduce infection of urinary catheters.

MATERIALS AND METHODS

Bacterial strains and growth conditions. Bacterial adhesion was evaluated using isogenic derivatives of the uropathogen *E. coli* C97, listed in Table 1, that differ in the production of colanic acid. *E. coli* C97 was collected from urine specimens of females (ages 7 to 15) in Götenborg, Sweden (6). Derivatives of this isolate were constructed by P1 transduction of mutations that are known to affect colanic acid production (3, 37). The strains named CPS wild type and CPS$^+$ were constructed by the same P1 transduction, selecting for transduction of the *ompC*::Tn*5* marker. Because the *rcsC137* mutation has 50% linkage to the *ompC* gene, we isolated cells that also cotransduced the *rcsC137* mutation (CPS$^+$) and those that did not cotransduce the *rcsC137* mutation (CPS wild type). The CPS$^-$ strain was constructed by transducing the cpsE::Tn*10* marker into the C97 parent strain. These mutations affect the *cps* genes such that transcription of the *cps* operon is either interrupted by a Tn*10* transposon (Cps$^-$) or increased approximately 1,000-fold with the *rcsC137* mutation (Cps$^+$). In order to evaluate the effect the disruption of *ompC* has on adhesion, an additional strain was created that only harbors *ompC*::Tn*5* (Cps WT).

Bacteria were grown in Luria-Bertani broth at 37°C with aeration. An overnight culture was used, diluted 1/100 into 250 ml of fresh Luria-Bertani broth, and grown to an optical density at 600 nm (OD_{600}) of 0.4 to 0.6 at 37°C. These exponential-phase cells were harvested, and the pellets were rinsed and resuspended in phosphate-buffered saline (PBS; pH 7.4) or Tris buffer (pH 7.4) to an OD_{600} of 2.5.

Substrate preparation. The substrates chosen for this study were glass coverslips (Erie Scientific Company, Portsmouth, N.H.). The coverslips were cleaned by soaking in 10% HNO_3 for at least 24 h followed by rinsing with distilled deionized water (ddH_2O) and methanol and air drying. Clean coverslips were made hydrophobic by treating with *N*-octadecyltrichlorosilane (OTS; Aldrich Chemical Company, Milwaukee, Wis.). Clean glass coverslips were immersed in 1% OTS–toluene for 2 to 3 h. The OTS-treated glass was then removed from the OTS solution and dipped into toluene to loosen unreacted OTS from the surface. Following OTS treatment, the slides retain patches of a white film consisting of polymerized OTS on the surface. OTS-treated coverslips were scoured with Alconox detergent to physically remove excess OTS. The Alconox scouring was performed by physically rubbing a small amount of Alconox on the surface of the coverslip until the white film was completely removed. OTS-treated coverslips were further cleaned by sonication in ddH_2O to remove any unreacted OTS from the surface. Sonication was carried out in multiple water baths until no OTS film was observed at the air-water interface. The coverslips were then stored in ddH_2O.

Silicone was prepared by using the Sylgard 184 silicone elastomer kit (Dow Corning, Midland, Mich.) with a 1/10 weight ratio of curing agent-elastomer. Silicone-coated coverslips were made by spin coating the silicone solution onto clean glass coverslips using a P6204-A spin coater (Specialty Coating Systems, Inc., Indianapolis, Ind.) at 7,000 rpm for 10 s. The coverslips were left to cure under ambient conditions for at least 24 h prior to use. A 100% silicone catheter manufactured by C. R. Bard, Inc. (Covington, Ga.) was maintained at 19°C in a Leica CM3050S cryostat (Bannockburn, Wis.). Interior sections of the silicone catheter were sliced to a thickness of 80 mm by embedding small sections of the catheter in Tissue-Tek tissue-embedding medium (Sakura Finetek USA, Inc., Torrance, Calif.). Catheter slices were rinsed three times with ddH_2O to remove any embedding medium prior to use. Slices were attached to glass coverslips for AFM and flow cell studies using double-sided adhesive (Digital Instruments, Santa Barbara, Calif.).

Zeta potential measurements. Zeta potentials were measured for bacteria in PBS buffer using a Zeta-Meter 3.0 (Zeta-Meter, Inc., Staunton, Va.) at a setting of 50 V/cm. Zeta potential measurements for each strain were repeated at least three times.

Contact angle measurements. Hydrophobicity of bacteria and planar substrates was evaluated by sessile drop contact angle measurements using a Ramé-Hart model 100-00 goniometer (Ramé-Hart, Inc., Mountain Lakes, N.J.). For the substrates, sessile drop contact angles were measured for probe liquids resting on the planar substrates. For bacteria, sessile drop contact angles were measured on bacterial lawns filtered onto membranes (5). Bacteria in Tris buffer were filtered onto 0.2-μm-pore-size nitrocellulose membranes (Pal Gelman Laboratory, Ann Arbor, Mich.) using a model 400-1901 vacuum pump (Barnant Company, Barrington, Ill.) until there was no liquid remaining over the filter. Contact angles for bacteria and substrates were measured using two polar liquids and one apolar liquid. The polar liquids were ddH_2O and 99.98% glycerol (spectrophotometric grade; EM Science, Gibbstown, N.J.), whereas the apolar liquid was 99.5% diiodomethane (Aldrich Chemical Co.). A drop of each of these liquids was placed on the substrate or bacterial cell lawn to measure the advancing contact angle (38). Contact angle measurements for the substrates and bacterial lawns were repeated at least three times.

AFM force measurements. A NanoScope E MultiMode AFM (Digital Instruments, Santa Barbara, Calif.) was used according to the protocol developed by Razatos et al. (32) to measure forces of interaction between bacteria immobilized on the tips of AFM cantilevers and planar substrates. In the protocol developed by Razatos et al. (31, 32), additional glutaraldehyde was added to the cells on the cantilever for 1 to 2 h in order to further fix the cells onto the polyethyleneimine-coated tips. In this study, the aforementioned protocol was modified by eliminating this final step of adding glutaraldehyde to the bacteria-coated cantilevers. Instead, the bacteria on the tips were incubated at room temperature for 15 min, rinsed with ddH_2O, and stored overnight at 4°C. Eliminating this step did not affect the stability of the bacterial lawns coating the cantilever tips. Extensive control studies have been carried out to insure that the immobilization protocol does not alter bacterial cell surface properties (i.e., hydrophobicity and surface charge density) and does not affect bacterial adhesion or AFM force measurements (30–32).

The AFM was operated by first engaging the cantilever close to, but not in contact with, the substrate in order to prevent contamination between the sample and the tip. The cantilever was carefully approached to the surface until contact. Once in contact, force measurements were recorded for a scan size of 200 nm at a rate of 1 Hz. Scanning electron microscopy (SEM) images were taken of the cantilevers after each experiment in order to ensure that bacteria were still present at the apex of the tips. Force curves for bacteria-coated cantilevers were compared to control curves for bare silicon nitride tips as another indicator that bacteria were on the tip during the AFM force measurement. To avoid sample contamination, cantilevers and substrates were used only once. At least three force measurements were obtained for each bacterial strain on each substrate.

Data analysis. Data were recorded by the NanoScope software version 4.43r5 (Digital Instruments) in terms of tip deflection (in nanometers) versus relative distance of separation (in nanometers). The slope of the portion of the curve where the cantilever moves with the surface (constant compliance region) was set equal to the rate of the piezo displacement. The beginning of the constant compliance region is the point of contact between bacteria and the surface (i.e., the zero point for the absolute distance of separation). Tip deflection (in nanometers) was converted to force (in nano-Newtons) by treating the cantilever as a spring with a characteristic spring constant according to Hooke's Law, $F = -k \cdot \Delta Y$, where ΔY is tip deflection and k is the spring constant of the cantilever. The spring constant of the long thin cantilevers used in this study ($k = 0.06$ N/m)

TABLE 2. Contact angle and zeta potential measurements for the *E. coli* C97 colanic acid mutant strains[a]

Strain	Contact angle with:			Zeta potential
	Water	Glycerol	Diiodomethane	
Cps^+	20.0 ± 3.4	19.1 ± 3.0	32.5 ± 3.9	−36.1 ± 5.3
Cps^-	24.0 ± 4.7	22.0 ± 4.2	62.5 ± 4.8	−27.6 ± 5.2
Cps WT	20.0 ± 3.6	18.6 ± 2.2	55.0 ± 4.1	−26.1 ± 4.0

[a] Data are means ± standard deviations.

was provided by the manufacturer (Digital Instruments). Force (in nano-Newtons) was then plotted versus the absolute distance of separation (in nanometers). Only the approach curves from AFM force measurements were considered in this study.

Parallel-plate flow cell studies. Bacterial adhesion was evaluated by standard flow cell studies using a parallel-plate flow cell apparatus. The parallel-plate flow cell (Bacterin, Bozeman, Mont.) consisted of a well (55 mm by 12 mm by 2 mm) enclosed by the transparent substrate. Fluid flow through the cell was driven by gravity. Bacteria harvested in exponential phase as described above were concentrated to an OD_{600} of 2.5 in PBS. Prior to injection into the flow cell, 0.5 ml of this cell suspension was mixed with 1 μl of the LIVE/DEAD *Bac*Light bacterial viability kit (Molecular Probes, Eugene, Oreg.) to fluorescently stain bacteria. A 0.5-ml aliquot of exponential-phase bacteria was then injected into the flow cell and incubated for 30 min. PBS buffer was flushed through the system at a flow rate of 7.5 ml/min for 15 min to rinse nonadherent cells. After rinsing, random areas within the flow cell were analyzed for adherent bacteria. The adherent bacteria within these randomly chosen quadrants were enumerated and photographed on a Nikon Eclipse TE300 (Nikon, Inc., Melville, N.Y.) inverted fluorescence microscope using a 100× objective. Black and white photographs of adhered fluorescent bacteria were taken in three fields of view using a Quantix 35-mm camera (Roper Scientific, Tucson, Ariz.). Bacterial cell counts were performed on three different locations within the flow cell chamber and averaged. Each experiment was repeated at least three times.

RESULTS

The physiochemical cell surface properties of the uropathogenic *E. coli* strains were characterized by zeta potential and contact angle measurements. Zeta potentials, which reflect cell surface charge density, are presented in Table 1 for the CPS wild-type, the CPS^+, and the CPS^- strains. Zeta potential measurements confirmed that all three strains are negatively charged. As expected, the CPS^+ strain, which continuously produces anionic colanic acid, was more negatively charged than the CPS wild-type and the CPS^- strains. The CPS wild-type and CPS^- strains do not produce colanic acid under normal laboratory growth conditions and, therefore, have similar surface charge densities. Contact angles, which reflect bacterial cell surface hydrophobicity, were also measured for the three bacterial strains. In brief, larger contact angles with polar probe liquids indicate that the surface is more hydrophobic. Conversely, larger contact angles with apolar probe liquids indicate that the substrate is less hydrophobic. Contact angles measured for the CPS wild-type, the CPS^+, and the CPS^- strains confirmed that all three strains are hydrophilic (Table 2). As expected, there was no difference in contact angle measurements between the CPS wild-type and CPS^- strains. The contact angle measured with diiodomethane for the CPS^+ strain was smaller than that measured for the CPS wild-type and CPS^- strains. This result indicates that the CPS^+ strain may be more hydrophobic than the other two strains. Therefore, although the colanic acid capsule renders CPS^+ more negatively charged, the capsule may interact less favorably with water molecules. This hypothesis, however, is not supported by contact angle measurements using water and glycerol.

Contact angles were also measured for the substrates under investigation, which included glass, OTS-treated glass, and spun-coated silicone (Table 3). Hydrophilic anionic glass and hydrophobic OTS-treated glass were chosen in this study to represent ideal, chemically defined substrates. Glass, with small contact angles, was strongly hydrophilic. OTS-treated glass and spun-coated silicone had large contact angles and were strongly hydrophobic. Silicone was included in this study because this hydrophobic material is commonly used to make urinary catheters. Bacterial adhesion on silicone was evaluated on spun-coated silicone substrates as well as thin slices of commercially available silicone catheters. The catheter slices were not uniform and, hence, difficult to work with. Nevertheless, results from AFM and parallel-plate flow cell studies were compared for spun-coated silicone versus sliced silicone catheter material to demonstrate that spun-coated silicone is an excellent model for silicone catheters.

AFM force measurements. The AFM was used to directly measure the physiochemical forces and specific binding interactions involved in the initial approach of uropathogenic *E. coli* bacteria to glass, OTS-treated glass, spun-coated silicone, and sliced silicone catheter material. The AFM-based methodology consisted of immobilizing bacteria directly onto the tip of standard AFM cantilevers. These cantilevers were then used to probe planar substrates in physiological solutions. The AFM cantilever was examined by SEM after each experiment to ensure that the tips were completely coated with bacteria. Figure 1 is an SEM micrograph of *E. coli* C97 bacteria immobilized on the tip of a standard AFM cantilever.

Clean glass was used in this study to represent an ideal hydrophilic substrate. As seen in Fig. 2A, all three *E. coli* strains (CPS wild type, CPS^+, and CPS^-) were repelled by glass in PBS buffer. These interactions are repulsive because the terminal force (force where the distance of separation is zero) is positive. A negative terminal force would indicate an attractive interaction. CPS wild type and CPS^- had similar repulsive interactions, whereas CPS^+ had a smaller repulsive interaction with glass (Fig. 2A). AFM force measurements with glass were repeated in higher electrolyte concentrations to reduce any electrostatic interactions. Addition of an electrolyte, such as NaCl, increases the counter-ion (Na^+) concentration and as a result decreases the double layer between two approaching surfaces (18). This decrease in double-layer thickness results in a decrease in electrostatic repulsion between two approaching charged surfaces (18). Figure 2B demonstrates that the addition of 100 mM NaCl to the PBS buffer reduced the repulsive interaction measured between clean glass and the CPS^- strain. Therefore, the repulsive force ini-

TABLE 3. Contact angle measurements of the substrates[a]

Substrate	Contact angle with:		
	Glass	OTS-treated glass	Spun-coated silicone
Water	10.6 ± 1.9	96.9 ± 12.0	109.8 ± 8.2
Glycerol	48.9 ± 6.8	85.4 ± 6.1	117.2 ± 6.3
Diiodomethane	43.3 ± 3.6	72.7 ± 9.2	79.3 ± 6.1

[a] Values are means ± standard deviations.

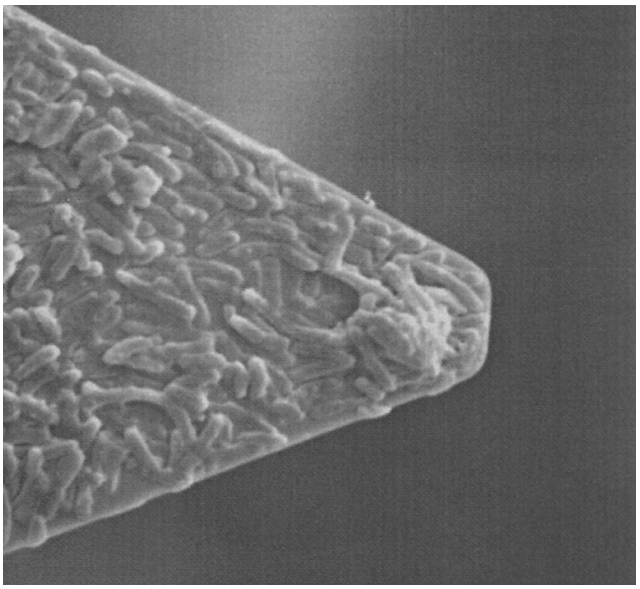

FIG. 1. SEM micrograph of an AFM cantilever tip coated with *E. coli* C97 bacteria.

tially measured between CPS^- and glass in PBS was due in part to electrostatic interactions. However, the addition of 1,000 mM NaCl to PBS did not further reduce the repulsive force measured between CPS^- and glass in the 100 mM NaCl–PBS solution (Fig. 2B). Therefore, the persistent repulsive force (~0.5 nN) measured in both 100 mM NaCl–PBS and 1,000 mM NaCl–PBS was not due to electrostatic interactions. Similar experiments were carried out for the CPS^+ strain. In this case, addition of 100 mM NaCl and 1,000 mM NaCl to PBS did not reduce the repulsive force between CPS^+ and glass in PBS shown in Fig. 2B (data not shown). Therefore, the repulsive interaction (~0.5 nN) between CPS^+ and glass was not electrostatic in nature. It is important to note that the forces measured by the AFM are not artifacts due to the deformation of bacteria. Previous AFM studies have shown that there is no apparent elastic deformation of bacterial cells immobilized onto glass substrates under the force of the AFM cantilever (30). Therefore, bacterial cells behave as rigid colloids during AFM force measurements as performed in this study.

Bacterial adhesion was evaluated on OTS-treated glass representing an ideal, chemically defined, hydrophobic substrate. The CPS wild-type and CPS^- strains were repelled by OTS-treated glass (Fig. 3). The small difference in force curves between the two strains was not statistically significant. The CPS^+ strain, on the other hand, was neither repelled nor attracted to OTS-treated glass (Fig. 3). Bacterial adhesion was also evaluated for spun-coated silicone and slices of silicone material. Spun-coated silicone and OTS-treated glass had similar contact angle measurements and, hence, were equally hydrophobic (Table 3). The AFM measured repulsive interactions between the spun-coated silicone and both the CPS wild-type and the CPS^+ strains (Fig. 4). Conversely, CPS^- was strongly attracted to silicone (Fig. 4). AFM measurements for the spun-coated silicone were compared to those for real silicone catheter material. AFM force measurements were identical for all strains on spun-coated and sliced silicone materials (data not shown).

Parallel-plate flow cell studies. Bacterial adhesion was also evaluated in a parallel-plate flow cell apparatus, which allowed for in situ observation and image analysis of bacteria adhering to planar substrates in solution. A parallel-plate flow cell apparatus was chosen for this study to model the flow of urine in a catheter. Flow cell studies were included to investigate the influence of colanic acid on bacterial adhesion during prolonged periods of incubation in comparison to AFM force measurements, which are instantaneous. The AFM directly measures the interaction forces as bacteria initially approach a substrate in less than 1 s. Conversely, a parallel-plate flow cell apparatus facilitates enumeration of bacteria adhering to a substrate for longer incubation times; in this case, bacteria were allowed to adhere for up to 30 min. The number of bacteria adhering to a substrate is an indirect measurement of the total force holding bacteria to a surface in the presence of shear flow. At this flow rate the hydrodynamic drag force acting on the bacteria, modeled as a sphere on a flat surface, is 2.5×10^{-13} N due to simple shear flow. In a flow cell device, bacteria adhere to substrates by both reversible physiochemical interactions (similar to those seen in the AFM measurements) and secondary, irreversible binding events.

The extent of adhesion was evaluated from photographs of bacteria adhering to the substrate-liquid interface in PBS buffer (Fig. 5). Results from flow cell studies are summarized in Table 4 for all strains and all substrates. The CPS wild-type and CPS^- strains that do not produce colanic acid adhered approximately 10-fold more efficiently to all substrates (Table 4). Relatively few CPS^+ cells adhered to any of the substrates in the flow cell (Table 4). No differences in bacterial cell counts were observed between silicone slices and spun-coated silicone for the three strains (Table 4).

DISCUSSION

E. coli bacteria secrete the exopolysaccharide colanic acid, which forms a slimy capsule surrounding the cell surface, under stressful conditions such as osmotic shock, low temperatures, and desiccation, indicating that the colanic acid capsule may function to protect bacteria in hostile environments (16, 20, 33-36, 42). Results from previous studies suggest that colanic acid inhibits bacterial adhesion (9, 14, 31). However, little is known about the physiochemical and/or specific binding interactions involved in the adhesion or repulsion of bacteria at a surface. AFM force measurements and flow cell experiments were carried out in this study to determine the role of physiochemical interactions (specifically, electrostatic and hydrophobic) and specific binding interactions during the initial adhesion of encapsulated and nonencapsulated cells in order to understand the events leading to urinary catheter infections.

Bacterial adhesion was evaluated for a series of isogenic uropathogenic *E. coli* strains that differ in the production of colanic acid (Table 1). One strain was constructed to constitutively express colanic acid capsule (CPS^+), and one was designed to never express capsule (CPS^-). The CPS^+ strain has a mutation in the regulatory gene, *rcsC*, and has a knockout mutation in the *ompC* gene. Because of this additional mutation, an isogenic strain was constructed for use as the control

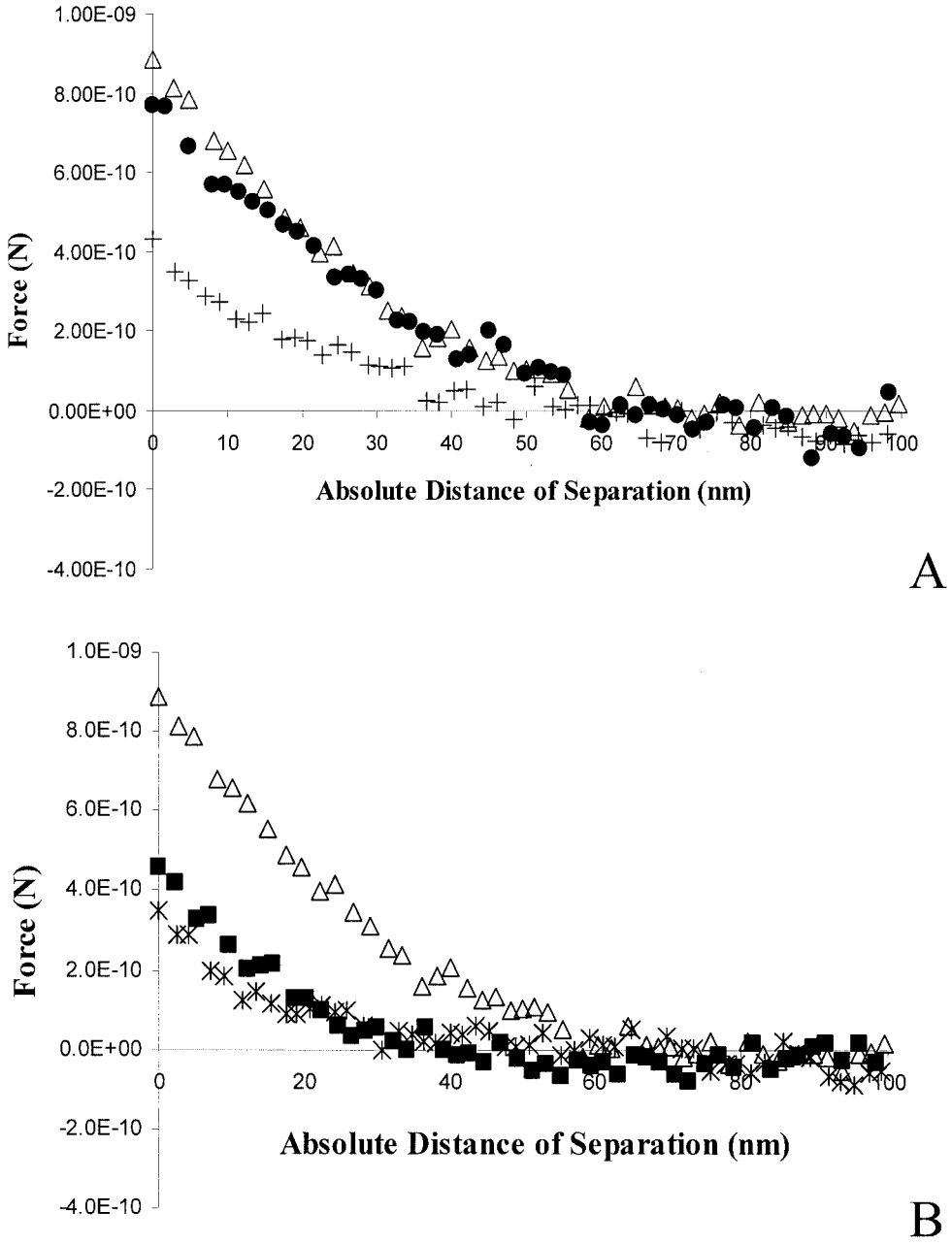

FIG. 2. AFM force-versus-distance curves of *E. coli* C97 bacteria interacting with hydrophilic glass. (A) CPS^+ (+), CPS wild-type (●), and CPS^- (△) strains in PBS buffer. (B) The CPS^- strain interacting with glass in PBS (△), PBS plus 100 mM NaCl (■), and PBS plus 1,000 mM NaCl (∗).

for the CPS^+ strain that has just the *ompC* mutation. This strain is designated the CPS wild type because it is wild type in colanic acid synthesis. The CPS^- strain has a knockout mutation in the *cpsE* gene, which is essential for colanic acid biosynthesis. The control for the CPS^- mutant was the C97 parent strain, which is wild type in colanic acid synthesis. Both the wild-type and the parent strains are capable of synthesizing colanic acid, although they do not produce it under normal laboratory growth conditions. In all of the experiments, the wild-type and the parent strains behaved identically, indicating that *ompC* does not affect adhesion. Therefore, data using the parent strain are not included. The CPS^+ strain synthesizes 500 to 1,000 times more colanic acid than the other three strains when they are grown under the conditions described in Materials and Methods. We cannot detect significant differences in the amount of colanic acid expression among the CPS^-, wild-type, and parental strains.

Bacterial adhesion was evaluated for the colanic acid mutant strains on anionic, hydrophilic glass to determine the role of electrostatic interactions. The AFM measured repulsive interactions between glass and both CPS wild-type and CPS^- strains (Fig. 2A). However, electrostatic interactions were only partially responsible for these repulsive interactions as demonstrated by AFM measurements performed in higher electro-

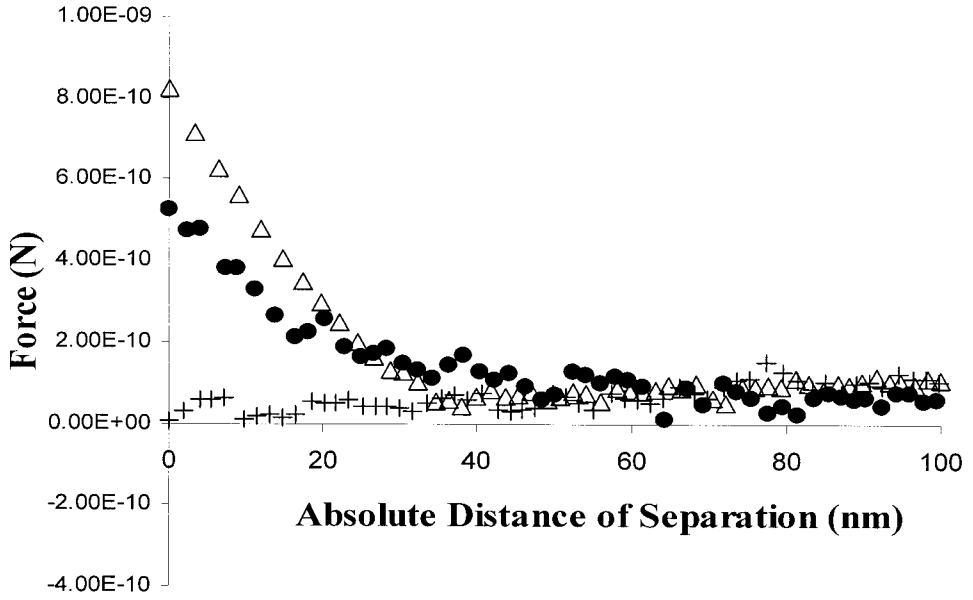

FIG. 3. AFM force-versus-distance curves of *E. coli* C97 bacteria interacting with hydrophobic OTS-treated glass. The CPS^+ (+), CPS wild-type (●), and CPS^- (△) strains were evaluated in PBS buffer.

lyte concentrations (Fig. 2B). AFM force measurements between glass and the CPS^+ strain were identical in PBS, PBS plus 100 mM NaCl, and PBS plus 1,000 mM NaCl (data not shown). Therefore, electrostatic interactions were not responsible for the repulsion between glass and CPS^+, even though the CPS^+ strain is more negatively charged than CPS wild type and CPS^-. Therefore, the AFM force measurements did not correlate with the surface charge densities of the three colanic acid mutant strains. A repulsive force (~0.5 nN) persisted between all three strains and glass even in the presence of high electrolyte concentrations. This force was not electrostatic and was therefore due to some other short-range physiochemical interaction, such as hydration pressure. Hydration pressure is due to short-range structural forces that usually appear at a separation distance of 4 nm (2, 25, 26); however, they have been observed at separations of 10 nm or more (21). While the origin and nature of hydration pressure is not completely understood, it appears to arise whenever water molecules bind to strongly hydrophilic materials (18), such as glass and bacterial cells. In addition to hydration pressure, cell surface structures may be responsible for the observed repulsive forces between the three strains and glass. Electron micrographs of the strains

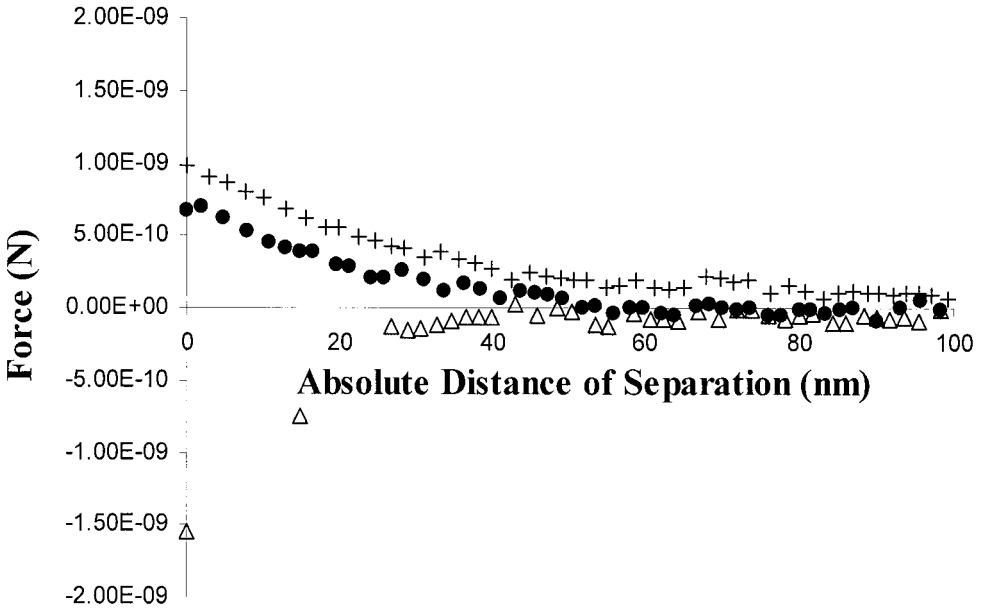

FIG. 4. AFM force-versus-distance curves of *E. coli* C97 bacteria interacting with hydrophobic silicone in PBS buffer. Interactions with spun-coated silicone were evaluated in CPS^+ (+), CPS wild-type (●), and CPS^- (△) strains.

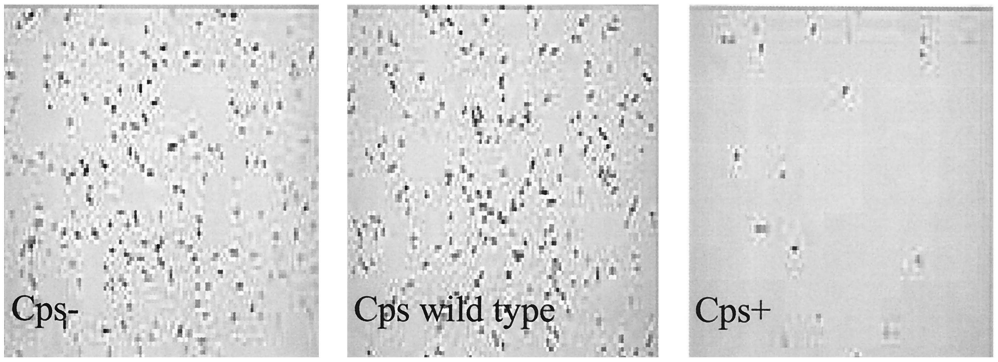

FIG. 5. Photographs of *E. coli* bacteria adhering to hydrophobic OTS-treated glass in PBS buffer in the parallel-plate flow cell apparatus.

revealed the presence of pilus-like structures on all three strains (data not shown). The identity of these structures remains to be determined.

OTS-treated glass was evaluated in this study to determine the contribution of hydrophobic interactions to adhesion. CPS wild type and CPS^- were both repelled by OTS-treated glass. CPS^+, which produced colanic acid and was more negatively charged, experienced neither a repulsive nor an attractive interaction with OTS. The 0.5-nN force measured between CPS^+ and clean glass was not detected between CPS^+ and OTS-treated glass. Based on contact angle measurements, a strong attractive interaction was expected between CPS^+ and hydrophobic OTS-treated glass. This discrepancy suggests that hydrophobic interactions did not play a significant role in the adhesion of the C97 colanic acid mutant strains.

If hydrophobic interactions were significant, then the CPS^+ strain should have been strongly attracted to silicone, which was also strongly hydrophobic. However, silicone repelled CPS^+ and CPS wild type. Conversely, the AFM measured a strong attractive force between CPS^- and silicone. Because hydrophobic interactions do not appear to play a significant role in adhesion of the C97 strains, this strong attraction between CPS^- and silicone was most likely due to some specific binding interaction. Specific binding is defined as a receptor-ligand-type interaction between molecules on the cell surface of CPS^- bacteria and silicone. The molecule or molecules responsible for this strong adhesive interaction between CPS^- and silicone remain to be resolved. OmpC was not found to be responsible for this specific binding, because both the CPS wild-type and the CPS parent strains were repelled by silicone—the repulsive curves were identical (data not shown). Two of the best candidates for these molecules are curli and pili, since they have been shown to affect adhesion in other model systems (27, 28).

Bacterial adhesion was evaluated for both spun-coated silicone and slices of actual silicone catheter material. Due to the soft nature of the catheter material, the microtome slices were rippled, which complicated AFM force measurements. Moreover, the rippled surface of the sliced silicone catheter material made it difficult to focus the inverted fluorescence microscope on the silicone-liquid interface during flow cell experiments. Spun-coated silicone was easy to work with because it was smooth, thin, and uniform. Both AFM and flow cell results in this study demonstrated that spun-coated silicone acts as an excellent model for silicone catheters and can be used with confidence in future studies on silicone catheter infections.

Results from AFM and flow cell studies were compared to determine if incubation time played a role in bacterial adhesion. In all cases, bacteria did not adhere to any of the substrates for incubation times less than 5 min. This observation is consistent with repulsive AFM force measurements, such as CPS wild type, CPS^+, and CPS^- interacting with glass. The lack of adhesion for times less than 5 min, however, was not consistent with the strong attractive force measured by the AFM between CPS^- and silicone. Bacteria were observed to begin adhering to substrates when incubation times were greater than 15 min. The data presented in Table 4 and Fig. 5 represent adhesion observed after 30 min of incubation. For example, significant adhesion of CPS wild type and CPS^- was observed on glass and OTS-treated glass in flow cell studies after 30 min of incubation. Conversely, these two strains were repelled by glass and OTS-treated glass during AFM force measurements. The AFM directly measures the interactions as bacteria initially approach a substrate, whereas flow cell experiments reflect the establishment of time-dependent interactions. Therefore, although OTS initially repelled bacteria, prolonged incubation resulted in surface colonization by the CPS wild-type and CPS^- strains. One possible explanation is that the repulsive forces initially measured by the AFM "relaxed" as a function of time, thus facilitating adhesion of CPS wild type and CPS^-. Another possible cause for the 15-min delay in adhesion time is that bacterial cell physiology was altered during the prolonged exposure of bacteria to the surface in the fluid cell.

According to AFM and flow cell studies, the CPS^+ strain that produced colanic acid did not adhere to any of the substrates evaluated in this study. Therefore, colanic acid appears

TABLE 4. Adhesion results from flow cell studies in terms of bacterial cell counts[a]

Substrate	Cps^+	Cps^-	Cps WT
Hydrophilic glass	10–30	230–280	260–300
Hydrophobic OTS glass	0–10	200–277	230–290
Spun-coated silicone	10–20	230–270	320–340
Silicone catheter	2–4	100–140	70–90

[a] Data are presented as the range of bacterial cell counts for at least three random microscopic fields (0.176 mm^2).

to interfere or block the time-dependent adhesion of bacteria to both hydrophilic and hydrophobic surfaces, as well as the specific binding to silicone catheter materials. Results from this study indicate that the capsular polysaccharide colanic acid does not enhance bacterial adhesion but rather blocks the establishment of specific binding as well as time-dependent interactions between bacteria and inert substrates. This suggests that *E. coli* devoid of colanic acid initially adheres to catheters and then expresses colanic acid during the development of mature biofilms.

ACKNOWLEDGMENTS

Acknowledgment is made to the donors of the Petroleum Research Fund, administered by the American Chemical Society, and the Whitaker Foundation Biomedical Engineering Research Grant Program for partial support of this research.

We also thank Dennis P. McDaniel in the W. M. Keck Bioimaging Laboratory for his assistance with fluorescence microscopy.

REFERENCES

1. **An, Y. H., and R. J. Friedman.** 1998. Concise review of mechanisms of bacterial adhesion to biomaterial surfaces. J. Biomed. Mater. Res. **43:**338–348.
2. **Basu, S., and M. M. Sharma.** 1996. Measurement of critical disjoining pressure for dewetting solid surfaces. J. Colloid Interface Sci. **181:**443–455.
3. **Brill, J. A., C. Quinlan-Walshe, and S. Gottesman.** 1988. Fine-structure mapping and identification of two regulators of capsule synthesis in *Escherichia coli* K-12. J. Bacteriol. **170:**2599–2611.
4. **Brooks, G., J. Butel, and S. Morse.** 1998. Jawetz, Melnick, and Adelberg's medical microbiology, 21st ed., p. 475. Appleton and Lange, Stanford, Calif.
5. **Busscher, H. J., A. H. Weerkamp, H. C. van der Mei, A. W. J. van Pelt, H. P. de Jong, and J. Arends.** 1984. Measurement of the surface free energy of bacterial cell surfaces and its relevance for adhesion. Appl. Environ. Microbiol. **48:**980–983.
6. **Caugant, D. A., B. R. Levin, G. Lidin-Janson, T. S. Whittam, C. Svanborg Eden, and R. K. Selander.** 1983. Genetic diversity and relationships among strains of Escherichia coli in the intestine and those causing urinary tract infections. Prog. Allergy **33:**203–227.
7. **Chomarat, M.** 2000. Resistance of bacteria in urinary tract infections. Int. J. Antimicrob. Agents **16:**483–487.
8. **Christensen, G. D., L. Baldassarri, and W. A. Simpson.** 1995. Methods for studying microbial colonization of plastics. Methods Enzymol. **253:**477–500.
9. **Christensen, G. D., W. A. Simpson, A. L. Bisno, and E. H. Beachey.** 1982. Adherence of slime-producing strains of *Staphylococcus epidermidis* to smooth surfaces. Infect. Immun. **37:**318–326.
10. **Christensen, T. E., O. Saxtrup, T. I. Hansen, B. H. Kristensen, B. L. Beck, T. Plesner, I. M. Krogh, V. Andersen, and S. Strandgaard.** 1983. Familial myoglobinuria. A study of muscle and kidney pathophysiology in three brothers. Dan. Med. Bull. **30:**112–115.
11. **Costerton, J. W., Z. Lewandowski, D. E. Caldwell, D. R. Korber, and H. M. Lappin-Scott.** 1995. Microbial biofilms. Annu. Rev. Microbiol. **49:**711–745.
12. **Costerton, J. W., Z. Lewandowski, D. DeBeer, D. Caldwell, D. Korber, and G. James.** 1994. Biofilms, the customized microniche. J. Bacteriol. **176:**2137–2142.
13. **Costerton, J. W., P. S. Stewart, and E. P. Greenberg.** 1999. Bacterial biofilms: a common cause of persistent infections. Science **284:**1318–1322.
14. **Danese, P. N., L. A. Pratt, and R. Kolter.** 2000. Exopolysaccharide production is required for development of *Escherichia coli* K-12 biofilm architecture. J. Bacteriol. **182:**3593–3596.
15. **Davenport, D. S., R. M. Massanari, M. A. Pfaller, M. J. Bale, S. A. Streed, and W. J. Hierholzer, Jr.** 1986. Usefulness of a test for slime production as a marker for clinically significant infections with coagulase-negative staphylococci. J. Infect. Dis. **153:**332–339.
16. **Gottesman, S., and V. Stout.** 1991. Regulation of capsular polysaccharide synthesis in *Escherichia coli* K-12. Mol. Microbiol. **5:**1599–1606.
17. **Gristina, A. G.** 1987. Biomaterial-centered infection: microbial adhesion versus tissue integration. Science **237:**1588–1595.
18. **Israelachvili, J.** 1992. Intermolecular and surface forces, 2nd ed. Academic Press Limited, San Diego, Calif.
19. **Ladd, T. I., D. Schmiel, J. C. Nickel, and J. W. Costerton.** 1987. The use of a radiorespirometric assay for testing the antibiotic sensitivity of catheter-associated bacteria. J. Urol. **138:**1451–1456.
20. **Nikaido, H., and M. Vaara.** 1987. Outer membrane, p. 7–22. *In* F. C. Neidhardt (ed.), *Escherichia coli* and *Salmonella*: cellular and molecular biology. ASM Press, Washington, D.C.
21. **Ninham, B.** 1999. On progress in forces since the DLVO theory. Adv. Colloid Interface Sci. **83:**1–17.
22. **Ochman, H., and R. Selander.** 1984. Standard reference strains of *Escherichia coli* from natural populations. J. Bacteriol. **157:**690–693.
23. **Ofek, I., and R. J. Doyle.** 1994. Bacterial adhesion to cells and tissues. Chapman Hall, Inc., New York, N.Y.
24. **Ohkawa, M., T. Sugata, M. Sawaki, T. Nakashima, H. Fuse, and H. Hisazumi.** 1990. Bacterial and crystal adherence to the surfaces of indwelling urethral catheters. J. Urol. **143:**717–721.
25. **Pashley, R.** 1980. Hydration forces between mica surfaces in aqueous electrolyte solutions. J. Colloid Interface Sci. **80:**153–162.
26. **Pashley, R. M.** 1981. DLVO and hydration forces between mica surfaces in Li, Na, K and Cs electrolyte solutions: a correlation of double-layer and hydration forces with surface cation exchange properties. J. Colloid Interface Sci. **83:**531–546.
27. **Pratt, L. A., and R. Kolter.** 1998. Genetic analysis of *Escherichia coli* biofilm formation: roles of flagella, motility, chemotaxis and type I pili. Mol. Microbiol. **30:**285–293.
28. **Prigent-Combaret, C., G. Prensier, T. T. Le Thi, O. Vidal, P. Lejeune, and C. Dorel.** 2000. Developmental pathway for biofilm formation in curli-producing Escherichia coli strains: role of flagella, curli and colanic acid. Environ. Microbiol. **2:**450–464.
29. **Prigent-Combaret, C., O. Vidal, C. Dorel, and P. Lejeune.** 1999. Abiotic surface sensing and biofilm-dependent regulation of gene expression in *Escherichia coli.* J. Bacteriol. **181:**5993–6002.
30. **Razatos, A., and G. Georgiou.** 2000. Evaluating bacterial adhesion using atomic force microscopy, p. 285. *In* Y. H. An and R. J. Friedman (ed.), Handbook for studying bacterial adhesion. Humana Press, Totowa, N.J.
31. **Razatos, A., Y. L. Ong, M. M. Sharma, and G. Georgiou.** 1998. Evaluating the interaction of bacteria with biomaterials using atomic force microscopy. J. Biomat. Sci. Polymer **9:**1361–1373.
32. **Razatos, A., Y. L. Ong, M. M. Sharma, and G. Georgiou.** 1998. Molecular determinants of bacterial adhesion monitored by atomic force microscopy. Proc. Natl. Acad. Sci. USA **95:**11059–11064.
33. **Roberts, I. S.** 1996. The biochemistry and genetics of capsular polysaccharide production in bacteria. Annu. Rev. Microbiol. **50:**285–315.
34. **Russo, T. A., G. Sharma, J. Weiss, and C. Brown.** 1995. The construction and characterization of colanic acid deficient mutants in an extraintestinal isolate of Escherichia coli (O4/K54/H5). Microb. Pathog. **18:**269–278.
35. **Sledjeski, D. D., and S. Gottesman.** 1996. Osmotic shock induction of capsule synthesis in *Escherichia coli* K-12. J. Bacteriol. **178:**1204–1206.
36. **Stout, V., and S. Gottesman.** 1990. RcsB and RcsC: a two-component regulator of capsule synthesis in *Escherichia coli.* J. Bacteriol. **172:**659–669.
37. **Trisler, P., and S. Gottesman.** 1984. *lon* transcriptional regulation of genes necessary for capsular polysaccharide synthesis in *Escherichia coli* K-12. J. Bacteriol. **160:**184–191.
38. **van Oss, C. J.** 1993. Acid-base interfacial interactions in aqueous media. Colloids Surfaces A **78:**1–49.
39. **Warren, J. W.** 1997. Catheter-associated urinary tract infections. Infect. Dis. Clin. North Am. **11:**609–622.
40. **Warren, J. W.** 1996. Urethral catheters, condom catheters, and nosocomial urinary tract infections. Infect. Control Hosp. Epidemiol. **17:**212–214.
41. **Warren, J. W., R. Platt, R. J. Thomas, B. Rosner, and E. H. Kass.** 1978. Antibiotic irrigation and catheter-associated urinary-tract infections. N. Engl. J. Med. **299:**570–573.
42. **Whitfield, C., and I. S. Roberts.** 1999. Structure, assembly and regulation of expression of capsules in Escherichia coli. Mol. Microbiol. **31:**1307–1319.